Shear Relaxation in Iron under the Conditions of Earth's Inner Core

A. B. Belonoshko,[1] T. Bryk,[2,3] and A. Rosengren[1]

[1]*Condensed Matter Theory, Department of Theoretical Physics, AlbaNova University Center, Royal Institute of Technology (KTH), 106 91 Stockholm, Sweden*

[2]*Institute for Condensed Matter Physics, National Academy of Sciences of Ukraine, 1 Svientsitskii Street, UA-79011 Lviv, Ukraine*

[3]*Institute of Applied Mathematics and Fundamental Sciences, National Polytechnic University of Lviv, UA-79013 Lviv, Ukraine*

(Received 9 March 2010; revised manuscript received 11 May 2010; published 16 June 2010)

Large scale molecular dynamics simulations of iron at high pressure and temperature are performed to investigate the physics of shear softening. A solid 16×10^6 atoms sample of iron is grown out of the liquid with a small solid immersed in it at the start of simulation. We observe that diffusion in the sheared solid is similar to that in liquid, even though at different time scales. This allows us to describe the time dependence of shear stress in terms of elastic and hydrodynamic relaxation. The elastic response of the sample is close to the elastic response of Earth's inner core. This explains the abnormally low shear modulus in the core. The reason for the low shear modulus is the presence of defects of the crystal structure.

DOI: 10.1103/PhysRevLett.104.245703 PACS numbers: 64.10.+h, 62.20.D−, 65.40.De

The standard approach to calculating elastic properties of a polycrystalline material consists in computing elastic constants of a single crystal and then averaging them according to some rule [1]. This approach, however, does not consider that crystals at high temperature are highly populated with various defects that might change their properties. Consideration of dislocations is helpful for the comparably low temperature materials, because at high temperature dislocations disintegrate for entropic reasons. The increasing number of defects is likely to affect mostly shear properties.

The most notorious failure of the averaging of the properties over ideal crystal orientations is its inability to explain the low shear modulus of Earth's inner core [2]. Earth's inner core (IC) material is mostly iron [3]. Indeed, the resistance of iron and its alloys to shear, either measured [4,5] or calculated [6], does not match the very low resistance to shear of the IC, as follows from the low velocity of the shear signal propagation [7,8]. The pressure (P) in the IC varies from 3.3 to 3.65 Mbar [7]. The melting temperature (T) of iron in the core was predicted to be above 7100 K [9,10] and the recent quantum Monte Carlo calculations [11] provided a melting T consistent with the earlier predictions. Some of the previous simulations predicted lower temperatures of iron melting at the $P =$ 3.3 Mbar (6600 ± 500 K and 6300 ± 100 K [12]). The most obvious reason for this discrepancy is that while the model in Ref. [10] was fitted to the all-electron first principles method data, the calculations that gave lower temperatures (not much lower, but still) relied on the explicit treatment of only 6 valence electrons. The question of the iron stable phase in the core is debated [13,14]. Recently, the stability of the body-centered cubic phase was indirectly confirmed by diamond-anvil cell (DAC) experiments [15]. Considering that addition of Si [16,17] makes the bcc phase more stable [18,19] while lowering the melting temperature of the hexagonal (hcp, the bcc competitor) phase [12], the likely phase of the material in the IC is bcc. Indeed, the anisotropy of seismic waves propagation in the IC [8] might be explained if the IC is bcc Fe and can not be explained if Fe is stable in hcp phase [20]. The hcp phase becomes isotropic at high temperature and the fcc, another proposed candidate, is isotropic by the virtue of the symmetry. Therefore, we have chosen to investigate the bcc iron phase at the pressure of the IC at temperatures close to melting (in the vicinity of 7000 K). The model we use (embedded atom method) is very well tested [2,10,13,20–24] and its use in the present study is well justified. The phase diagram of the model and comparison to experimental data are provided in Ref. [13] (Fig. 4).

Our plan was to simulate a very large system that would contain an equilibrium number of defects. For that purpose, we have chosen the method of molecular dynamics (MD) to simulate the process of crystallization, similar to the approach used in the studies of Xe [25]. First, we simulated the liquid phase of iron starting from the bcc structure. The initial structure was obtained by a $200 \times 200 \times 200$ translation of the bcc unit cell containing 2 atoms. Then, we applied the temperature of 12 000 K and pressure of 3.65 Mbar maintaining the cubic shape but allowing volume to change during MD simulation. During the equilibration stage the temperature was maintained by velocity scaling. After obtaining the liquid structure, it was thermalized at 7000 K and 3.65 Mbar by applying Berendsen thermo- and barostat. This is only 300 ± 100 degrees lower than the melting temperature, so no solidification took place [the corresponding radial distribution function (RDF) is typical of a liquid, as shown in Fig. 1]. After that, a 400 thousand atoms bcc sample was immersed in the center of the liquid box (the sample was presimulated at the

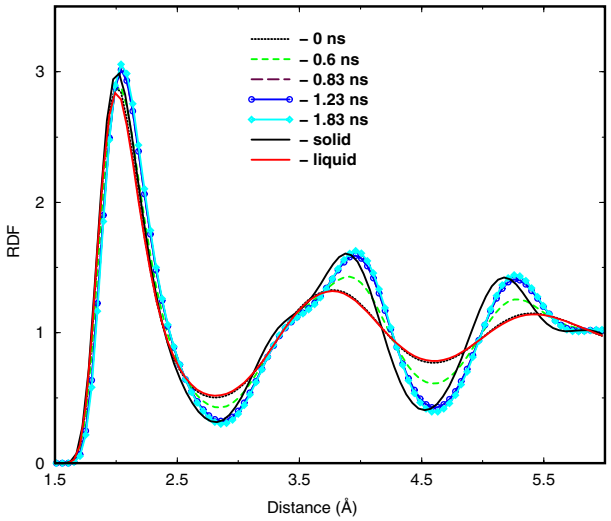

FIG. 1 (color online). Radial distribution functions of the initially two-phase system (bcc sample immersed in liquid) at different stages of solidification (the time from the start of simulation is indicated in legend) compared to liquid (thick curve) and solid (thin curve) at $P = 365$ GPa and $T = 7000$ K.

same P and T as for the liquid). The "liquid" atoms that overlap with the solid sample were removed. Thus, we obtained a two-phase system and, starting from 7200 K and 3.65 Mbar, that is just under the melting conditions [10], we began MD simulations in the NVE ensembles. The cutoff of the potential was chosen at 6.0 Å. Tests with higher cutoffs show negligible changes. The time step was equal to 0.0005 ps. The solid sample in the center of the box started to grow, temperature went up (due to the heat of crystallization) and pressure went down (because of the higher density of the solid phase). As soon as the simulation arrived at a point on the melting curve and crystallization stopped, the simulation was restarted at a slightly lower temperature and the whole process was repeated. Eventually, we obtained a completely solid (bcc) sample with defects that appear naturally during crystal growth. The final temperature was about 6700 K and the pressure was around 3.4 Mbar. The initial, final, and intermediate structures are shown in Fig. 1. One can see that the starting structure is typical of a liquid. After about 0.8 ns the structure becomes solid. Still we run the simulation for another nanosecond (2×10^6 time steps) to ensure that nonequilibrium defects are annealed. The next step is to shear the sample and measure the shear resistance.

The sample, that was a cube with an edge of about 50 nm, was sheared by 1 nm. The shear was applied in such a way that the "new" atom coordinates in the deformed sample were obtained from the "old" coordinates according to the formula $X_{\text{new}} = X_{\text{old}} + Yd/L$, $d = 1$ nm is the shear magnitude and L is the size of the cubic box ($\approx$50 nm). Such a shear corresponds to the strain normally applied to calculate C_{44}. Then, we performed the MD simulation of this sample keeping constant shape and temperature of 6700 K applying the Berendsen thermostat. This strain is definitely within the elastic limit for an ideal crystal. The sheared structure was simulated for 0.32 ns, recording the mobility of atoms (Fig. 2) and shear modulus (Fig. 3) (computed as the negative stress divided by strain).

The shear modulus is no longer constant and changes over time (Fig. 3) (the shear stress was averaged every 100 time steps to get the "instant" shear stress). This is in contrast to the case of ideal bcc structure, where the shear stress is strictly constant. Eventually, the shear modulus becomes lower than in the IC (about 200 GPa [7]). However, what is the mechanism behind such a behavior? We note that the mobility of atoms in the sheared solid sample (Fig. 2) is similar to their mobility in liquid, though the time scale is different. Certain differences are, of course, there: note the shoulder on the mobility curves for solids. The shoulder appears due to the lattice quantized mobility; however, it is a rather minor feature. Therefore, we decided to describe the stress relaxation in a way similar to the approach applied for liquids.

Generalized shear viscosity and shear relaxation for liquids can be well described by generalized hydrodynamics [26]. The simplest viscoelastic dynamic model for transverse dynamics yields for transverse mass current a two-exponential expression [27] for the correlation decay:

$$F_{JJ}(k, t) = A_h e^{-z_h(k)t} + A_k e^{-z_k(k)t}, \quad (1)$$

where the first term corresponds to the hydrodynamic process of shear relaxation, whereas the second term represents nonhydrodynamic (kinetic) effects in dynamics. The wave-number-dependent inverse relaxation times $z_i(k)$ are expressed as follows:

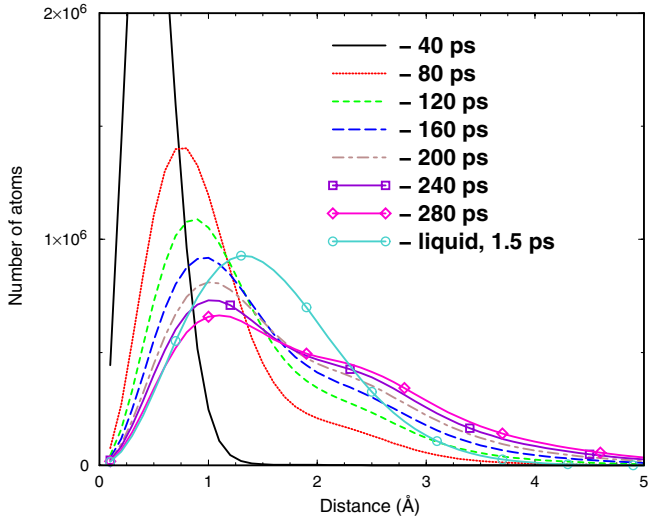

FIG. 2 (color online). Mobility of atoms (defined as the distance that an atom traveled from its position in the starting configuration) at different times in the sheared sample. The mobility in liquid is provided for comparison. Note the shoulder that develops in the solid at a larger distance. This shoulder is likely due to the structure modulated by the lattice.

(i) hydrodynamic relaxation

$$z_h(k) = \frac{\eta k^2}{\rho}, \tag{2}$$

where η is shear viscosity, ρ is mass density;

(ii) kinetic elastic relaxation

$$z_k(k) = \frac{G}{\eta} - \frac{\eta k^2}{\rho}, \tag{3}$$

where G is shear modulus. When $k \to 0$, i.e., on macroscopic distances in liquids $z_h(k) \ll z_k(k)$, and only the hydrodynamic mechanism of shear relaxation is important, that also prohibits the propagation of shear waves on macroscopic distances. Only on nanoscales, corresponding to some wave number k_s such that $z_h(k_s) \approx z_k(k_s)$, the shear waves can emerge in the liquid.

One can formally apply expression (1) to a finite sample by associating its length L with a characteristic wave number $k = 2\pi/L$. Hence the relaxation times are

(i) for hydrodynamic decay

$$\tau_h = \frac{\rho L^2}{4\pi^2 \eta}, \tag{4}$$

(ii) for elastic decay

$$\tau_k = \frac{\eta \rho L^2}{G\rho L^2 - 4\pi^2 \eta^2}. \tag{5}$$

Now, let us assume that on large time scales the solid behaves as a liquid. Indeed, we see that at times of approximately 100 ps and more, the mobility of atoms in the solid is comparable to that in the liquid (Fig. 2). In a solid, at short times both elastic and viscous response can contribute to the shear modulus. However, only elastic response can facilitate the propagation of the transverse wave.

Therefore, we will describe the time dependence of the shear modulus by the equation

$$G(t) = G_e e^{-t/t_e} + G_v e^{-t/t_v}, \tag{6}$$

where G_e and G_v are the elastic and viscous parts of the shear modulus at $t = 0$, and t_e and t_v are the characteristic times of elastic and viscous response. Indeed, the time dependence of the shear modulus can be very well described by Eq. (6) (Fig. 3).

The important implication is that the elastic response of iron in the IC is significantly smaller than the shear response in total. However, it is the elastic response that provides propagation of the transverse wave. The instant shear modulus at time 0 that belongs to the nondissipating part of the elastic response of iron to the strain is about 280 GPa (Fig. 3). This is higher than 200 GPa deduced from seismic measurements, although it is significantly lower than 392 ± 10 GPa for the ideal bcc crystal. The difference between 200 and 280 GPa can be attributed to a

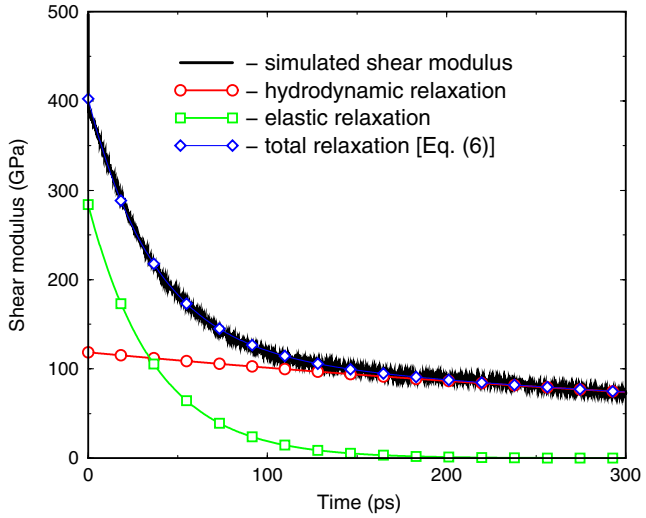

FIG. 3 (color online). Time dependence of the shear modulus (defined as the negative of stress divided by strain) in the sheared sample (in an ideal crystal the shear corresponds to the c_{44} elastic constant). The shear is equal to 0.02. The modulus is fitted with the 2 exponent expression (Eq. (6)) with an extremely small error of fitting. Each exponential term is also shown separately.

temperature in the IC higher than 6700 K, alloying with light elements, and grain boundaries. The impact of the latter can be dramatic [2,28].

The time scale of the hydrodynamic relaxation might have implication for the DAC experiments. In some of these experiments very low melting temperatures have been measured, much lower than in shock-wave experiments. The time scales of these experiments are very different. It is possible that the regime of dynamic recrystallization might have been erroneously considered as a melting [29] in DAC experiments. The L^2 dependence of the time required for the hydrodynamic processes in solid allows us to estimate that if the time scale of measurements in DAC is larger than $\approx 10^{-4}$ s, the results of these measurements might be due to movements caused by yielding related to the shear softening. However, if the heating is performed by the so-called pulsed method [30] on a time scale of 10^{-6} s, melting will not be confused with the shear flow.

Concluding, we want to emphasize that our study was performed in the true spirit of computer experimental work. We synthesized the required sample, subjected it to shear, and recorded the measurements. Having insight into the details unparalleled in any other approach, we have been able to explain the softening of iron, and this may explain the low shear modulus of the material in Earth's inner core.

Computations were performed using the facilities at the Swedish National Infrastructure for Computing (SNIC). The use of DL_POLY 3.06 code [31] is gratefully acknowledged. A. R. acknowledges support from the Swedish

Research Council (VR).

[1] W. Voigt, *Lehrbuch Der Kristallphysik* (Teubner-Verlag, Leipzig, 1928).

[2] A. B. Belonoshko, N. V. Skorodumova, S. Davis, A. N. Ospitsov, A. Rosengren, and B. Johansson, Science **316**, 1603 (2007).

[3] R. J. Hemley and H.-K. Mao, Int. Geol. Rev. **43**, 1 (2001).

[4] D. Antonangeli *et al.*, Earth Planet. Sci. Lett. **225**, 243 (2004).

[5] H.-K. Mao *et al.*, Nature (London) **396**, 741 (1998).

[6] L. Vocadlo, Earth Planet. Sci. Lett. **254**, 227 (2007).

[7] A. M. Dziewonski and D. L. Anderson, Phys. Earth Planet. Inter. **25**, 297 (1981).

[8] A. Cao, B. Romanowicz, and N. Takeuchi, Science **308**, 1453 (2005).

[9] A. B. Belonoshko and R. Ahuja, Phys. Earth Planet. Inter. **102**, 171 (1997).

[10] A. B. Belonoshko, R. Ahuja, and B. Johansson, Phys. Rev. Lett. **84**, 3638 (2000).

[11] E. Sola and D. Alfe, Phys. Rev. Lett. **103**, 078501 (2009).

[12] M. J. Gillan, D. Alfe, J. Brodholt, L. Vocadlo, and G. D. Price, Rep. Prog. Phys. **69**, 2365 (2006).

[13] A. B. Belonoshko, R. Ahuja, and B. Johansson, Nature (London) **424**, 1032 (2003).

[14] L. Voĉadlo *et al.*, Nature (London) **424**, 536 (2003).

[15] A. B. Belonoshko, P. M. Derlet, A. S. Mikhaylushkin, S. I. Simak, O. Hellman, L. Burakovsky, D. C. Swift, and B. Johansson, New J. Phys. **11**, 093039 (2009); A. S. Mikhaylushkin, S. I. Simak, L. Dubrovinsky, N. Dubrovinskaia, B. Johansson, and I. A. Abrikosov, Phys. Rev. Lett. **99**, 165505 (2007).

[16] J. P. Pourier, Phys. Earth Planet. Inter. **85**, 319 (1994).

[17] C. J. Allegre, J. P. Pourier, E. Humler, and A. W. Hofmann, Earth Planet. Sci. Lett. **134**, 515 (1995).

[18] A. B. Belonoshko, A. Rosengren, L. Burakovsky, D. L. Preston, and B. Johansson, Phys. Rev. B **79**, 220102(R) (2009).

[19] F. W. Zhang and A. R. Oganov, Geophys. Res. Lett. **37**, L02305 (2010).

[20] A. B. Belonoshko, N. V. Skorodumova, A. Rosengren, and B. Johansson, Science **319**, 797 (2008).

[21] S. V. Starikov and V. V. Stegailov, Phys. Rev. B **80**, 220104 (R) (2009).

[22] C. Desgranges and J. Delhommelle, Phys. Rev. B **76**, 172102 (2007).

[23] D. K. Belashchenko, N. E. Kravchunovskaya, and O. I. Ostrovski, Inorg. Mater. **44**, 939 (2008).

[24] L. Koci, A. B. Belonoshko, and R. Ahuja, Phys. Rev. B **73**, 224113 (2006).

[25] A. B. Belonoshko, R. Ahuja, and B. Johansson, Phys. Rev. Lett. **87**, 165505 (2001); A. B. Belonoshko, Phys. Rev. B **78**, 174109 (2008).

[26] J.-P. Boon and S. Yip, *Molecular Hydrodynamics* (McGraw-Hill, New-York, 1980).

[27] T. Bryk and I. Mryglod, J. Phys. Condens. Matter **12**, 6063 (2000).

[28] C. Zener, Phys. Rev. **60**, 906 (1941).

[29] A. B. Belonoshko, R. Ahuja, and B. Johansson, Phys. Rev. B **61**, 11928 (2000).

[30] S. Deemyad and I. F. Silvera, Phys. Rev. Lett. **100**, 155701 (2008).

[31] I. T. Todorov, W. Smith, K. Trachenko, and M. T. Dove, J. Mater. Chem. **16**, 1911 (2006).